Dyes and Pigments 88 (2011) 18–24

Contents lists available at ScienceDirect

Dyes and Pigments

journal homepage: www.elsevier.com/locate/dyepig

Nonlinear optical properties and memory effects of the azo polymers carrying different substituents

Najun Li [a], Jianmei Lu [a,*], Hua Li [a], En-Tang Kang [b,**]

[a] Key Laboratory of Organic Synthesis of Jiangsu Province, College of Chemistry, Chemical Engineering and Material Science, Suzhou University, Suzhou, Jiangsu 215123, China
[b] Department of Chemical and Biomolecular Engineering, National University of Singapore, 10 Kent Ridge, 119260 Singapore

ARTICLE INFO

Article history:
Received 5 January 2010
Received in revised form
26 April 2010
Accepted 26 April 2010
Available online 20 May 2010

Keywords:
Azo
Polymer
Substituent
Nonlinear optical
Electric memory
Device

ABSTRACT

The third-order nonlinear optical properties and electric memory behavior of azobenzene polymers were influenced by different substituents. The nonlinear optical coefficients of polymer films measured using the Z-scan technique revealed that the polymers with different substituents exhibited different nonlinear absorption. The reversibility of sandwich memory devices based on the azobenzene polymers was dependant on the terminal substituent on the azobenzene chromophore. Polymers with electron-accepting terminal moieties in the azobenzene pendant showed write-once-read-many-times memory whereas the polymer that contained electron-donating moieties displayed a FLASH-type (rewritable) memory.

1. Introduction

In recent years, azobenzene-containing polymers have received much attention owing to their potential application in optical data storage, nonlinear optical (NLO) materials, holographic memories and waveguide switches [1–8]. Besides optical manipulation, some reports have demonstrated the potential of azobenzene molecules to function as molecular switches at the nanoscale level [9–11]. In addition, electric memories based on voltage-induced electric bistability of polymers containing an azobenzene main chain group have also been described [12,13]. The current research group has reported the NLO properties of azo polymers [14–17]. In this work, a series of azo monomers containing different electron donor or acceptor groups and their polymers (**PAzo**s) were synthesized. The third-order NLO coefficients of the polymers were measured using the Z-scan technique; the voltage-induced electrical switching behavior and associated memory behavior of devices comprising **PAzo** films sandwiched between an indium-tin-oxide (ITO) bottom electrode and an Al top electrode are also reported.

2. Experimental

2.1. Materials

N-ethyl-N-(2-hydroxyethyl) aniline (Tokyo Kasei Kogyo Co. Ltd. in Japan, 98%) and ethyl 2-bromoisobutyrate (EBiB) (Acros, 99%) were used as received. 4-Nitroaniline, 4-bromoaniline, 4-methoxyaniline and triethylamine were all purchased from Shanghai chemical reagent Co. Ltd. as analytical regents and used without further purification (declared purity grade, ≥99%). Methacryloyl chloride was produced by Haimen Best Fine Chemical Industry Co. Ltd. and used after redistillation. N,N,N′,N″,N″-pentamethyldiethylenetriamine (PMDETA) (Jiangsu Liyang Jiangdian Chemical Factory, 98%) was dried with molecular sieve and distillated. Copper (I) bromide (CuBr) (A.R., Shanghai Zhenxin Chemical Reagent Factory) was purified with sodium sulfite and glacial acetic acid and stored under argon atmosphere at room temperature. Tetrahydrofuran (THF), cyclohexanone and N,N-dimethyl formamide (DMF) were purified by reduced pressure distillation. Other reagents were commercially available and used as received.

2.2. Instruments for characterization

FTIR spectra were recorded on a Perkin–Elmer 577 FTIR spectrophotometer in KBr disks. Elemental analysis was performed by

* Corresponding author. Tel./fax: +86 512 65882875.
** Corresponding author. Tel./fax: +65 6516 2189.
E-mail addresses: lujm@suda.edu.cn (J. Lu), cheket@nus.edu.sg (E.-T. Kang).

0143-7208/$ – see front matter © 2010 Elsevier Ltd. All rights reserved.
doi:10.1016/j.dyepig.2010.04.010

Italian 1106FT analyzer. ^{1}H NMR spectra of monomers and polymers in $CDCl_3$ were obtained on an Inova 400 MHz FT-NMR spectrometer at ambient temperature. The UV–Vis absorption spectra were carried out at room temperature in the region of 190–700 nm with a UV-1601 spectrophotometer using cell path lengths of 0.5 cm. Molecular weights (M_n) and polydispersity (M_w/M_n) were measured on a gel permeation chromatography (GPC) utilizing Waters 515 pump and differential refractometer. THF was used as a mobile phase at a flow rate of 1.0 M min^{-1}. The glass transition temperature (T_g) values of the azo polymers were determined on a 2010 DSC TA Instrument at a heating rate of 10 K min^{-1} under nitrogen atmosphere. The surface morphology of the films was examined by atomic force microscopy (AFM) using an SPA 400 system from Seiko Instruments Inc., Japan. Scanning electron microscope (SEM) cross-section images of the memory device were taken on a Hitachi S-4700 equipped with an energy-dispersive X-ray spectrum (EDS).

2.3. Synthesis of azo monomers and their homopolymers

The three monomers namely, 4′-[N-(2-methacryloyloxy ethyl)-N-ethyl] amino-4-nitro azobenzene (**NAzo**), 4′-[N-(2-methacryloyloxy ethyl)-N-ethyl] amino-4-bromo azobenzene (**BAzo**) and 4′-[N-(2-methacryloyloxy ethyl)-N-ethyl] amino-4-methoxy azobenzene (**MAzo**) were synthesized following a procedure that was modified from that described in the literature [18,19], as shown in Scheme 1. Atom transfer radical polymerization (ATRP) was successfully used to prepare the homopolymers with controlled number-average M_r and low polydispersity. Each polymer was prepared using ethyl 2-bromoisobutyrate (EBiB), CuBr, and N,N,N′,N″,N″-pentamethyldiethylenetriamine (PMDETA) as initiator, catalyst and ligand, respectively.

2.3.1. NAzo

^{1}H NMR ($CDCl_3$): δ(ppm) = 8.31 (d, 2H, ArH–NO_2), 7.94–7.90 (d, 4H, ArH), 6.81 (d, 2H, ArH), 6.11 (s, 1H, =CH_2), 5.59 (s, 1H, =CH_2), 4.39 (t, 2H, –OCH_2), 3.72 (t, 2H, H_2C–N), 3.53 (m, 2H, –CH_2), 1.94 (s, 3H, –OCH_3), 1.27 (t, 3H, –CH_3). ($C_{20}H_{22}N_4O_4$) (382.4): Calcd. C 62.816, H 5.7983, N 14.651, Found C 62.636, H 5.9426, N 14.516. UV–Vis (DMF): $\lambda_{max}(\varepsilon)$ = 465 nm (1300 L mol^{-1} cm^{-1}).

2.3.2. BAzo

^{1}H NMR ($CDCl_3$): δ(ppm) = 7.88–7.73 (d, 4H, ArH), 7.60 (d, 2H, ArH–Br), 6.82 (d, 2H, ArH), 6.11 (s, 1H, =CH_2), 5.58 (s, 1H, =CH_2), 4.38 (t, 2H, –OCH_2), 3.71 (t, 2H, H_2C–N), 3.50 (m, 2H, –CH_2), 1.94 (s, 3H, –CH_3), 1.25 (t, 3H, –CH_3). ($C_{20}H_{22}N_3BrO_2$) (416.3): Calcd. C 57.701, H 5.3261, N 10.093, Found C 57.588, H 5.4812, N 9.8862. UV–Vis (DMF): $\lambda_{max}(\varepsilon)$ = 416 nm (1750 L mol^{-1} cm^{-1}).

2.3.3. MAzo

^{1}H NMR ($CDCl_3$): δ (ppm) = 7.83–7.81 (d, 4H, ArH), 6.98 (d, 2H, ArH–OCH_3), 6.80 (d, 2H, ArH), 6.09 (s, 1H, =CH_2), 5.57 (s, 1H, =CH_2), 4.34 (t, 2H, –OCH_2), 3.70 (s, 3H, –OCH_3), 3.66 (t, 2H, H_2C–N), 3.48 (m, 2H, –CH_2), 1.93 (s, 3H, –CH_3), 1.23 (t, 3H, –CH_3). ($C_{21}H_{25}N_3O_3$) (367.4): Calcd. C 68.644, H 6.857, N 11.436, Found C 68.987, H 6.8526, N 11.524. UV–Vis (DMF): $\lambda_{max}(\varepsilon)$ = 405 nm (1200 L mol^{-1} cm^{-1}).

2.3.4. PNAzo

M_n = 4500, M_w/M_n = 1.27 (GPC, polystylene calibration). ^{1}H NMR ($CDCl_3$): δ(ppm) = 8.4–8.2 (ArH–NO_2), 7.9–7.7 (ArH), 6.8–6.7 (ArH), 4.3–3.9 (–OCH_2), 3.8–3.6 (–CH_2), 2.0–1.4 (–CH_3), 1.2–0.8 (–CH_3 and –CH_2). UV–Vis (DMF): $\lambda_{max}(\varepsilon)$ = 470 nm (1450 L mol^{-1} cm^{-1}). T_g = 142 °C.

2.3.5. PBAzo

M_n = 5350, M_w/M_n = 1.26 (GPC, polystylene calibration). ^{1}H NMR ($CDCl_3$): δ(ppm) = 7.9–7.6 (ArH), 7.6–7.45 (Br–ArH), 6.8–6.6 (ArH), 4.2–3.8 (–OCH_2), 3.6–3.2 (–CH_2), 2.0–1.4 (–CH_3), 1.2–0.8 (–CH_3 and –CH_2). UV–Vis (DMF): $\lambda_{max}(\varepsilon)$ = 420 nm (1800 L mol^{-1} cm^{-1}). T_g = 120 °C.

2.3.6. PMAzo

M_n = 5500, M_w/M_n = 1.27 (GPC, polystylene calibration). ^{1}H NMR ($CDCl_3$): δ (ppm) = 7.8–7.6 (ArH), 6.9–6.75 (ArH–OCH_3), 6.75–6.6 (ArH), 4.3–4.1 (–OCH_2), 3.9–3.7 (–OCH_3), 3.6–3.2

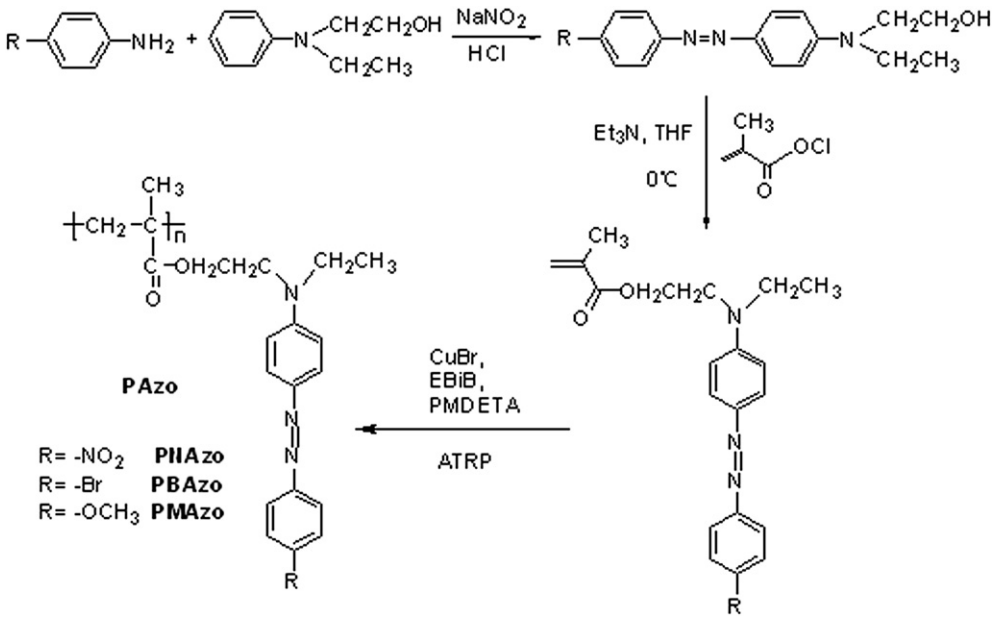

Scheme 1. Synthetic route of the azo monomers and homopolymers containing different substituted azobenzene side chains.

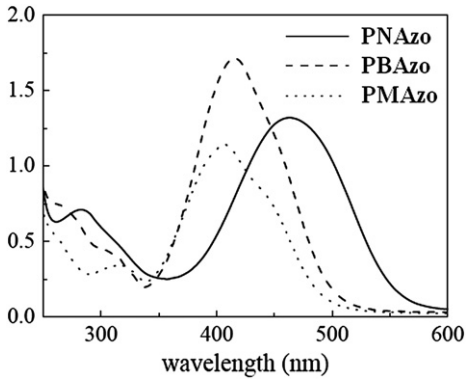

Fig. 1. UV–Vis spectra of azo homopolymers containing different substituted azobenzene side chains.

(−CH_2), 2.0–1.6 (−CH_3), 1.3–0.7 (−CH_3 and −CH_2). UV–Vis (DMF): $\lambda_{max}(\varepsilon) = 409$ nm (1400 L mol^{-1} cm^{-1}). $T_g = 112$ °C.

2.4. Preparation of polymer films and the third-order NLO measurement

Appropriate amounts of polymer were dissolved in freshly distilled DMF to give 25% w/w solutions. After filtration through 0.2 μ filter, films were prepared by spin-coating the solution on quartz glass. The prepared glass slides were placed in a vacuum chamber at 60 °C for 24 h to remove residual solvent, resulting in a film thickness of ~0.5 μm, as measured using an alpha-step profilometer. The third-order NLO coefficients of the azo polymer films were measured using the Z-scan technique [20–22] using a Continuum Q-switched Nd:YAG laser system from which produces 4 ns (Full width at half-maximum) laser pulses at 532 nm with a repetition rate of 1 Hz. The single pulse incident energy is about 1.0 μJ. The input and output energies of the pulses were measured simultaneously with two energy detectors (laser Precision Rjp-765) controlled by computer. Before measurement for **PAzo** films, carbon disulfide (CS_2) is taken as a reference to rectify the Z-san optical path.

2.5. Fabrication and measurement of memory devices based on *PAzo*

The memory devices consisting of the **PAzo** films sandwiched between an indium-tin-oxide (ITO) bottom electrode and an Al top electrode were fabricated. The N,N′-dimethylacetamide (DMAc) solution of **PAzo** (10 mg mL^{-1}) was spin-coated (2000 rps) onto ITO-coated glass and the solvent was removed in a vacuum chamber at 10^{-5} torr at 60 °C for 10 h. Finally, a layer of Al was thermally evaporated and deposited onto the polymer surface at about 10^{-7} torr through a shadow mask to form the top electrode and so as to define an active cross-area of 0.4 × 0.4 mm^2. All electrical measurements of the devices were characterized, under ambient condition without any encapsulation, using a Hewlett–Packard 4156A semiconductor parameter analyzer equipped with an Agilent 16440A SMU/pulse generator and a Keithley 4200-SCS semiconductor characterization system connected to a Cascade probe station with a microchamber and hot chuck. Cyclic voltammetry was carried out by Chi 604c electrochemical analysis to evaluate the reduction and oxidation (redox) behavior of each azo polymer.

3. Results and discussion

3.1. Material properties

The good solubility in a wide range of organic solvents and the T_g value of each polymer above 100 °C indicates that these azobenzne-containing homopolymers are promising for solid-state applications in NLO and electric memory devices. As shown in Fig. 1, the UV–Vis spectrum of each azo polymer exhibits two major absorption peaks. The absorption peak at the shorter wavelength is attributed to the π–π* electronic transition of aromatic ring while the peak at the longer wavelength is due to the π–π* electronic transfer of the azo bond. The polymers with different terminal electron donor and acceptor groups in the azobenzene side chains exhibit significant positive solvatochromic shift for the lowest energy π–π* transition.

3.2. Third-order NLO properties

In our experiment, the third-order NLO coefficients of the synthetic azo polymer films were investigated utilizing Z-scan technique with a single-beam method, which can obtain the nonlinear absorption and nonlinear refraction simultaneously [23–26]. It can be seen from Fig. 1 that **PBAzo** and **PMAzo** have hardly linear absorbance at 532 nm, which promises low intensity loss and little temperature change by photon absorption during the NLO measurements. But **PNAzo** has a little linear absorbance at 532 nm. In order to avoid the accumulative intensity loss and heating effect by linear absorption of **PNAzo**, all the azo polymer films were measured with a low input energy (1.0 μJ) and a repetition rate of 1 Hz.

The results of Z-scan with and without an aperture showed that all the azo polymers have both nonlinear absorption and nonlinear

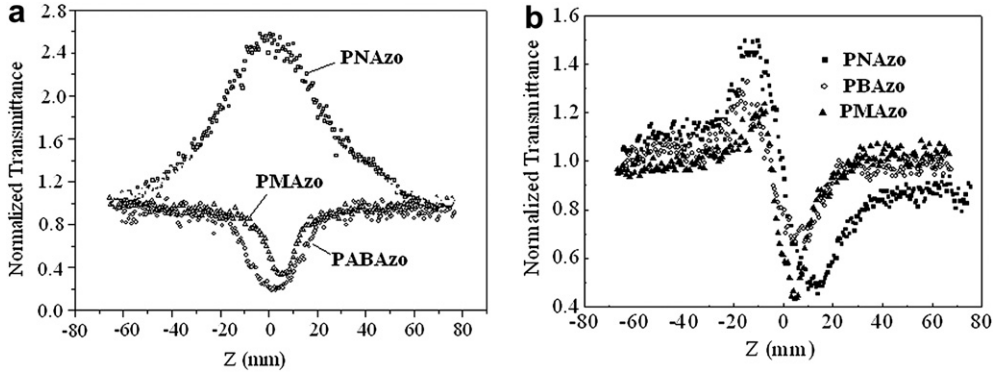

Fig. 2. (a) Normalized open-aperture Z-scan curves and (b) normalized transmittance curves of the azobenzene-containing acrylates and their polymers.

Table 1
Third-order NLO coefficients of azo-containing polymers in film state.

PAzo	T_0[a]	β ($\times 10^{-8}$ m W^{-1})	n_2 ($\times 10^{-17}$ m^2 W^{-1})
PNAzo	0.56	−4.75	−15.1
PBAzo	0.61	3.24	−9.8
PMAzo	0.63	3.01	−9.3

[a] T_0 is the linear transmittance of the samples.

refraction. The nonlinear absorption coefficient β can be determined through the fitting of the experimental data based on *Eq.* (1)–(2) [20],

$$T(z, s = 1) = \sum_{m=0}^{\infty} \frac{[-q_0(z)]^m}{(m+1)^{3/2}}, \text{ for } |q_0| < 1 \quad (1)$$

$$q_0(z) = \beta I_0(t) L_{\text{eff}} / \left(1 + Z^2/Z_0^2\right) \quad (2)$$

Here β is the nonlinear absorption coefficient, $I_0(t)$ is the intensity of laser beam at focus ($z = 0$), $L_{\text{eff}} = [1 - \exp(-\alpha_0 L)/\alpha_0]$ is the effective thickness with α_0, the linear absorption coefficient and L, the sample thickness, z_0 is the diffraction length of the beam, and z is the sample position.

The nonlinear refractive component of the sample was obtained by dividing the normalized Z-scan measured under a closed aperture configuration by the normalized Z-scan data obtained under the open-aperture configuration. Thus, the refractive curves were obtained. The third-order nonlinear refractive index, n_2, could be got by fitting the refractive curves using *Eq.* (3):

$$n_2 = \frac{\alpha_0 \lambda \Delta T_{p-v}}{0.812\pi I_0 (1-s)^{0.25}\left[1 - e^{-\alpha_0 L}\right]} \quad (3)$$

where $\Delta T_{p-v}$is the measured peak–valley transmittance difference from a normalized Z-scan curve, I_0 is the on-axis peak intensity at the focus ($z = 0$), s is the transmittance of the aperture ahead the detector in absence of a sample. Here, s is 0.13.

The open-aperture experimental Z-scan curves of azo polymers with different substituents are shown in Fig. 2(a). The normalized energy transmittance of **PNAzo** increases at the focus indicating a saturated absorption (SA) ($\beta < 0$), while **PBAzo** and **PMAzo** display reverse saturated absorption (RSA) ($\beta > 0$). It is caused by the different electronic effects of the substituent on the azobenzene chromophore. As electron withdrawing nitro-group substituted in the azobenzene system, the π-electron conjugation is enhanced obviously and the absorption cross-section of its excited state is smaller than that of ground state under the irradiation of 532 nm laser, which caused saturated absorption [27,28]. The peak–valley pattern of the normalized transmittance curves in Fig. 2(b) indicated that each of the azobenzene-containing polymers had a negative sign for the nonlinear refraction and exhibited a strong self-defocusing behavior. The third-order NLO coefficients of **PAzo**s were calculated by equations and listed in Table 1. The nitro-substituted polymer (**PNAzo**) film has the largest coefficients of the nonlinear absorption (β) and nonlinear refraction (n_2) values because a push–pull (D–π–A) electron system is formed by the electron withdrawing nitro-substituent with dimethylamino-group in the azobenzene side chain, which enhances the delocalization effect and is favorable to increase the NLO effect.

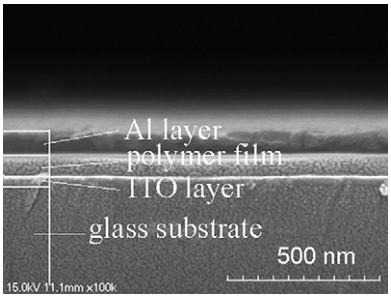

Fig. 4. Cross-section SEM image of the device ITO/**PNAzo**/Al device.

3.3. Electrical characterization of *PAzo*-based memory devices

Electrical transitions in the ITO/**PAzo**/Al devices were observed by measuring the current response to an external applied voltage. ITO was maintained as the ground electrode in all electrical measurements. The surfaces of the fabricated azo polymer films were all observed under AFM. A typical AFM image of polymer film and the schematic diagram of the memory devices are shown in Fig. 3. It showed that the surface of the film is flat and clean, no sign of any phase separation was observed. In order to confirm the polymer film continuity across the interface in the sandwiched device, a SEM cross-section image of ITO/**PAzo**/Al was investigated. As shown in Fig. 4, each layer of the memory device (ITO/**PNAzo**/Al) is clear and the polymer film continuity across the interface is good. In addition, we can make an estimate of the thickness of each layer (ITO film on glass, polymer film and Al layer). The polymer film is about 50–70 nm and the aluminum top layer is about 80–100 nm.

The current density–voltage (J–V) curves of the ITO/**PNAzo**/Al in Fig. 5(a) show two distinct conductivity states. The device is initially in the low-conductivity (OFF) state with a current density of about 10^{-6} A cm^2 when a voltage sweep was applied starting from 0 to 1.0 V. When the negative voltage was increased further (from 0 to 1.5 V), the device switches from the OFF-state to the high-conductivity (ON) state at a threshold voltage of about −1.5 V, as indicated by the abrupt increase of the current density to about

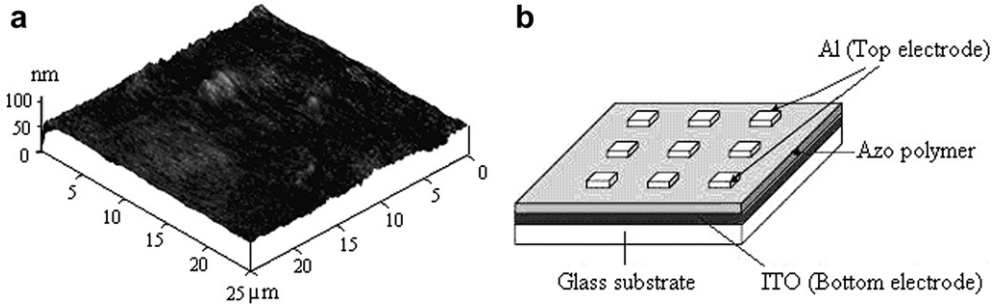

Fig. 3. (a) Topographical AFM image of a **PNAzo** film spin-coated on ITO-glass substrate and (b) the schematic diagram of the memory device consisting of a thin film of azo polymer sandwiched between ITO and Al electrodes.

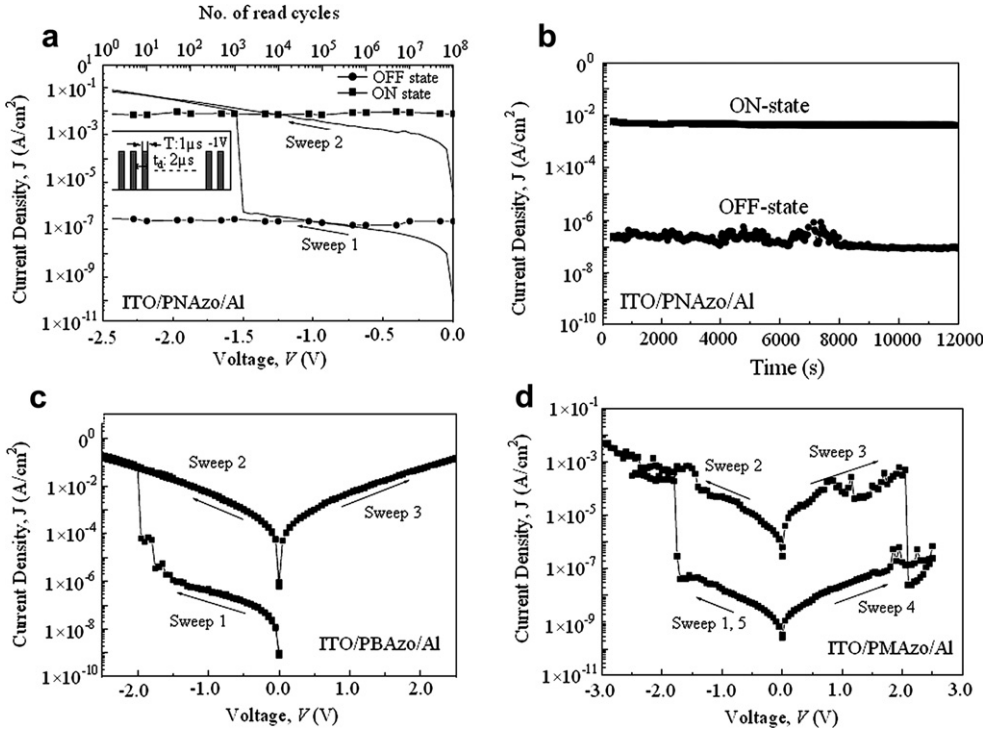

Fig. 5. (a) Current density–voltage (J–V) characteristics, (b) effect of operation time (at −1.0 V) on the device current density in the OFF- and ON-states of ITO/**PNAzo**/Al device, (c) current density–voltage (J–V) characteristics of ITO/**PBAzo**/Al WORM device and (d) current density–voltage (J–V) characteristics of ITO/**PMAzo**/Al FLASH device.

10^{-1} A cm^2 (Sweep 1). The high current density observed during the subsequent voltage sweep indicates retention of the ON-state in the device (Sweep 2). The ON-state J–V curves under negative and opposite biases were symmetrical. The transition from the OFF-state to the ON-state serves as the "writing" process for the memory device. The ON-state of the device could be distinguished from the OFF-state by an ON/OFF current ratio of about 10^4 when read at −1.0 V. After undergoing the OFF-to-ON transition, ITO/**PNAzo**/Al remain in its ON-state even after electrical power has been turned off and cannot be returned to the low-conductivity state by applying a reverse bias. This behavior is characteristic of a write-once-read-many-times (WORM) memory device. The ON- and OFF-states of the device is stable for up to 10^8 continuous read pulses of −1.0 V (pulse period = 2 μs, pulse width = 1 μs) without any resistance degradation. The retention ability at the OFF- and ON-states of this device is tested by first subjecting a device in the OFF-state to a constant voltage stress of −1.0 V and recording the current passing through the device at regular intervals. The device is then programmed by a voltage sweep and the ON-state is evaluated under the same stress condition. Fig. 5(b) shows that the ITO/**PNAzo**/Al device has both stable OFF- and ON-state currents within 3 h, with the high ON/OFF current ratio sustained.

The electrical switching behavior and the retention ability of another azo polymer device, ITO/**PBAzo**/Al, is also investigated. The bromo group also possesses electron-accepting properties but is a weaker acceptor in comparison with the nitro moiety. As shown in Fig. 5(c), the behavior of ITO/**PBAzo**/Al is of WORM type, with a switching threshold voltage of −1.9 V and an ON/OFF current ratio of about 10^4. The stability of the two conductivity states (OFF-state and ON-state) of the WORM device is demonstrated by the almost constant current densities observed when the device was placed under constant voltage stress for a period exceeding 3 h.

When the nitro terminal moiety in the azobenzene side chain of the polymer was replaced by the methoxy group, different electrical behaviors were observed. As the ITO/**PMAzo**/Al device, an abrupt increase in the current density was observed at about −1.7 V when a voltage sweep from 0 to −3.0 V was applied (Sweep 1), as shown in Fig. 5(d). The high-conductivity ON-state was retained when the voltage sweep was applied again (Sweep 2). In a voltage sweep of opposite bias from 0 to 3.0 V (Sweep 3), an abrupt decrease in the current density was observed at a threshold voltage of about 2.0 V, indicating the device transition from the ON-state back to the OFF-state. This electrical transition represents the "erase" process for the memory device. The device remains in the OFF-state during the following positive sweep (Sweep 4). The "erased" state can be further converted to the "written" state when the switching threshold voltage was re-applied, indicating that the memory device was rewritable (Sweep 5). Both the low- and the high-conductivity (OFF and ON) states of the device were stable under power-off conditions and under constant voltage stress conditions of −1.0 V, as well as maintaining an ON/OFF current ratio of about 10^4 when read at −1.0 V. The ability of the device to undergo write, read and erase cycles fulfills the functionality of a FLASH-type memory device.

From the above electrical characteristics of **PAzo**s, we can see that the memory type of the ITO/**PAzo**/Al device is affected by the electron accepting or donating of the terminal substitutent on azobenzene chromophore. We did some experiments to discuss the physical meaning of the electrical behaviors of the ITO/**PAzo**/Al devices. The UV–Vis spectroscopy and cyclic voltammetry of three

Table 2
High-occupied-molecular-orbital (HOMO) and lowest-unoccupied-molecular-orbital (LUMO) energy levels obtained from cyclic voltammetry and UV–Vis spectroscopy.

PAzo	HOMO (eV)	LUMO (eV)	HOMO → ITO (eV)	Al → LUMO (eV)	Threshold voltage (V)
PNAzo	5.53	3.30	0.73	0.98	−1.5
PBAzo	5.54	2.96	0.74	1.32	−1.9
PMAzo	5.45	2.77	0.65	1.51	−1.7

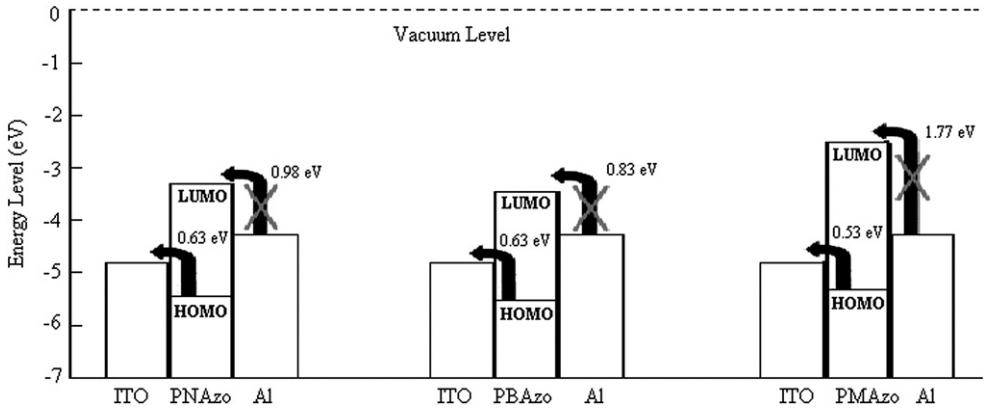

Fig. 6. Schematic energy diagram of ITO/**PAzo**/Al devices.

azo polymers were investigated to obtain the experimental values of HOMO and LUMO (Table 2) according to the method reported [29,30]. Based on an analysis of the barrier heights from charge injection to the electrodes (work function of ITO = 4.8 eV, work function of aluminum = 4.28 eV), the barrier to hole injection from ITO electrode is smaller compared to the barrier to hole injection from the Al electrode. So charge injection into the polymer layer via hole injection from ITO to the HOMO of each polymer is more favorable under the applied negative bias, as shown in Fig. 6. The azo polymers become *p*-doped under the induction of the electric field and switches to the high-conductivity state (ON-state). Correspondingly, the devices based on azo polymers exhibit OFF-to-ON transitions when a negative bias is applied. The threshold voltage value of each polymer is coincident with their E_g value. Bigger the E_g of the azo polymer is, higher its threshold voltage is (**PBAzo**> **PMAzo**> **PNAzo**). It can be considered that bigger the E_g is, more charges are requisite to be injected into the polymer layer to overcome the energy barrier, so the OFF-to-ON threshold voltage is in a higher negative value.

4. Conclusion

A series of polymers with azobenzene pendant containing different electron donor and acceptor were prepared. All of the azo polymers have both nonlinear absorption and nonlinear refraction and the third-order optical nonlinearities are influenced by the electronic effect of the different substituents on the azobenzene group. The electron withdrawing nitro-substituent which form a push–pull (D–π–A) electron system with dimethylamino-group and enlarge π-conjugation system in the azobenzene molecule is favorable to increase the NLO susceptibility values. The volatility of the memory effect is also determined by the electronic effect of the donor/acceptor on the end of polymer side chain. WORM memory effect is observed in the memory device based on the azo polymers whose side chain containing nitro or bromo (acceptor) terminal moieties, while FLASH-type memory effect is observed in the device based on the azo polymer containing methoxy (donor) terminal moieties.

Acknowledgements

This work is supported by the National Natural Science Foundation of China (Grant No. 20876101, 20902065) and the Natural Science Foundation of the Jiangsu Higher Education Institutions of China (Grant No. 09KJB430010).

References

[1] Perry JW, Mansour K, Lee IYS, Wu X, Bedworth PV, Chen C, et al. Organic optical limiter with a strong nonlinear absorptive response. Science 1996;273:1533–6.
[2] Ichimura K. Photoalignment of liquid–crystal systems. Chem Rev 2000; 100:1847–74.
[3] Hagen R, Bieringer T. Photoaddressable polymers for optical data storage. Adv Mater 2001;13:1805–10.
[4] Liu YG, Jiang AG, Xiang L, Gao J, Huang DY. Nonlinear optical chromophores with good transparency and high thermal stability. Dyes Pigm 2000;45(3): 189–93.
[5] Chen XB, Zhang JJ, Zhang HB, Jiang ZH, Shi G, Li YB, et al. Preparation and nonlinear optical studies of a novel thermal stable polymer containing azo chromophores in the side chain. Dyes Pigm 2008;77(1):223–8.
[6] Wang DR, He YN, Deng W, Wang XG. The photoinduced surface-relief-grating formation behavior of side-chain azo polymers with narrow M_r distribution. Dyes Pigm 2009;82(3):286–92.
[7] Meng X, Natansohn A, Barrett C, Rochon P. Azo polymers for reversible optical storage. 10. Cooperative motion of polar side groups in amorphous polymers. Macromolecules 1996;29:946–52.
[8] Labarthet FL, Bruneel JL, Buffeteau T, Sourisseau C. Chromophore orientations upon irradiation in gratings inscribed on azo-dye polymer films: a combined AFM and confocal Raman microscopic study. J Phys Chem B 2004;108: 6949–60.
[9] Alemani M, Peters MV, Hecht S, Rieder KH, Moresco F, Grill L. Electric field-induced isomerization of azobenzene by STM. J Am Chem Soc 2006;128: 14446–7.
[10] Yasuda S, Nakamura T, Matsumoto M, Shigekawa H. Phase switching of a single isomeric molecule and associated characteristic rectification. J Am Chem Soc 2003;125:16430–3.
[11] Attianese D, Petrosina M, Vacca P, Concilio S, Iannelli P, Rubina A, et al. Switching device based on a thin film of an azo-containing polymer for application in memory cells. IEEE Electron Device Lett 2008;29(1):44–6.
[12] Ling QD, Kang ET, Neoh KG, Chen Y, Zhuang XD, Zhu CX, et al. Thermally stable polymer memory devices based on a π-conjugated triad. Appl Phys Lett 2008;92:143302.
[13] Ponomarev YV, Ivanov SA, Rumyantsev YA, Gromchenko AA. Dynamics of photoinduced dichroism and birefringence in optically thick azopolymers. Quantum Electron 2009;39(1):46–52.
[14] Li NJ, Lu JM, Xu QF, Xia XW, Wang LH. Synthesis of optical-active azo-containing acrylates using atom transfer radical polymerization under microwave irradiation. Eur Polym J 2007;43:4486–92.
[15] Li NJ, Lu JM, Xu QF, Xia XW, Wang LH. Atom transfer radical polymerization and third-order nonlinear optical properties of New azobenzene-containing side-chain polymers. Macromol Chem Phys 2007;208:399–404.
[16] Li NJ, Lu JM, Xu QF, Wang LH. Synthesis and the third-order non-linear optical properties of new azobenzene-containing side-chain polymers. Opt Mater 2006;28:1412–6.
[17] Li NJ, Lu JM, Yao SC. Synthesis and optical properties of a new series of side-chain poly(amic acid)s with p–π conjugation. Macromol Chem Phys 2005;206:559–65.
[18] Natansohn A, Rochon P, Gosselin J, Xie S. Azo polymers for reversible optical storage. 1. Poly[4′-[[2-(acryloyloxy)ethyl]ethylamino]-4-nitroazobenzene]. Macromolecules 1992;25:2268–73.
[19] Li NJ, Lu JM, Xia XW, Xu QF, Wang LH. Synthesis of third-order nonlinear optical polyacrylates containing an azobenzene side chain via atom transfer radical polymerization. Dyes Pigm 2009;80:73–9.
[20] BaHae MS, Said AA, Wei TH. Sensitive measurement of optical nonlinearities using a single beam. IEEE J Quantum Electron 1990;26:760–9.

[21] Audebert P, Kamada K, Matsunaga K, Ohta K. The third-order NLO properties of D–π–A molecules with changing a primary amino group into pyrrole. Chem Phys Lett 2003;367:62–71.
[22] Yin SC, Xu HY, Shi WF, Gao YC, Song YL, Lam JWY, et al. Synthesis and optical properties of polyacetylenes containing nonlinear optical chromophores. Polymer 2005;46:7670–7.
[23] Su XY, Guang SY, Xu HY, Liu XY, Li S, Wang X, et al. Controllable preparation and optical limiting properties of POSS-based functional hybrid nanocomposites with different molecular architectures. Macromolecules 2009;42:8969–76.
[24] Su XY, Xu HY, Guo QZ, Shi G, Yang JY, Song YL, et al. Stilbene-containing polyactylenes: molecular design, synthesis, and relationship between molecular structure and NLO properties. J Polym Sci Polym Chem 2008; 46:4529–41.
[25] Yin SC, Xu HY, Shi WF, Bao L, Gao YC, Song YL, et al. Preparation and optical properties of poly(4-ethynyl-4′-[*N*,*N*-diethylamino]azobenzene-*co*-phenylacetylene). Dyes Pigm 2007;72:119–23.
[26] Yin SC, Xu HY, Su XY, Wu L, Song YL, Tang BZ. Preparation and property of soluble azobenzene-containing substituted poly(1-alkyne)s optical limiting materials. Dyes Pigm 2007;75:675–80.
[27] Liu Z, Tian J, Zhang W, Zhou W, Song F, Zhang C. Flexible alteration of optical nonlinearities of iodine charge-transfer complexes in solutions. Opt Lett 2004;29(10):1099–101.
[28] Louri EB, Nikifor R, Glauco SM, Cid BA. Changes in porphyrin nonlinear absorption owing to interaction with bovine serum albumin. Appl Opt 2000; 39(24):4431–5.
[29] Bredas JL, Silbey R, Boudreaux DS, Chance RR. Chain-length dependence of electronic and electrochemical properties of conjugated systems: polyacetylene, polyphenylene, polythiophene, and polypyrrole. J Am Chem Soc 1983;105:6555–9.
[30] Lee YZ, Chen XW, Chen SA, Wei PK, Fann WS. Soluble electroluminescent poly (phenylene vinylene)s with balanced electron- and hole injections. J Am Chem Soc 2001;123:2296–307.